Solid state spatially resolved ^{1}H and ^{19}F nuclear magnetic resonance spectroscopy of dental materials by stray-field imaging

C. H. LLOYD*, S. N. SCRIMGEOUR*‡, G. HUNTER‡, J. A. CHUDEK‡
*Dundee Dental School and ‡Chemistry Department, University of Dundee, Dundee, UK
D. M. LANE, P. J. MCDONALD
Physics Department, University of Surrey, Guildford, UK

As part of a program to evaluate the use of stray-field magnetic resonance microimaging (STRAFI) in dental materials research spatially resolved nuclear magnetic resonance (NMR) for solid dental cements has been investigated. By applying a quadrature echo pulse sequence to a specimen positioned in the stray-field of a NMR spectrometer superconducting magnet the magnetic resonance within a thin slice was obtained. The specimen was stepped through the field in 500 μm increments to record ^{1}H and ^{19}F profiles and T_2 values at each point. The specimens were fully cured cylinders made from four types of restorative material (glass ionomer, resin modified glass ionomer, compomer, composite). The values for ^{1}H T_2 varied with material type and reflected the nature of the matrix structure. For all materials containing ^{19}F in the glass two values were calculated for ^{19}F T_2, one short and one long. These were relatively invariant. Solid state magic angle spinning (MAS)-NMR showed that they came from the glass. This suggests that a proportion of the element is relatively mobile (in a glass phase) and the remainder is more tightly bound (in a compound dispersed in the glass). This demonstration, that NMR microimaging of both ^{1}H and ^{19}F in solid dental cements is possible, opens up exciting new possibilities for investigating the distribution of these elements (in particular fluorine) in solid dental materials.

1. Introduction

1.1. Magnetic resonance microimaging applied to dental materials

When a material is placed in a homogeneous magnetic field nuclear spins will align and the nuclei will possess a resonance frequency dependent upon the field strength, the gyromagnetic ratio of the element (specifically a particular isotope), and its chemical environment. In conventional magnetic resonance spectroscopy the nuclei are excited by a coherent broad-band pulse of radio frequency energy. This causes the magnetism (of the nuclei) to rotate away from the direction of the spectrometer magnetic field then dephase. The detected signal is known as the free induction decay (FID). To obtain spatial resolution it is necessary to superimpose a time dependent linear gradient magnetic field. This causes the resonance frequency to change in a linear way along the gradient. The optimum spatial resolution, Δx is [1]

$$\Delta x = \frac{2}{T_2 \gamma g_x} \quad (1)$$

where γ is the gyromagnetic ratio of the nucleus, T_2 the spin–spin relaxation time and g_x the gradient field strength. The spin–spin relaxation time, T_2, is dependent upon the structure of the material. In molecules that are small and relatively mobile T_2 is long (e.g. up to seconds for ^{1}H in free water). As the mobility becomes more restricted (e.g. ^{1}H in elastomeric polymers) or a substructure creates a restriction (e.g. ^{1}H in water in biological materials) T_2 shortens to a few milliseconds. In solids (e.g. ^{1}H in glassy polymers) T_2 is shorter still, measured in microseconds.

The line shape observed in spectroscopy is the Fourier transform of the FID. Hence, if T_2 is long the resonance peak is sharp and fine resolution is obtained in magnetic resonance imaging since it is possible to resolve peaks which are closely spaced. In conventional magnetic resonance microimaging (MRM) instrumentation and pulse sequences are optimized to give a high resolution in a small sample. For biological samples rich in water it is possible to produce a ^{1}H image with $10 \times 10 \times 100\,\mu m^3$ voxels using a 7 T homogeneous static magnetic field with a $1\,T\,m^{-1}$ field gradient [1]. If T_2 is short, as is the case in solids, a broader peak (often many kHz wide) is produced. This effectively renders

Corresponding author: Charles Lloyd, Dundee Dental School, University of Dundee, Dundee, Scotland, DD1 4HN, UK

solids non-imaging when conventional MRM instrumentation is used. To produce the same resolution in non-biological solid materials would require much higher field gradients to compensate for shorter T_2 values (see Equation 1). Unfortunately limits are imposed by the production of large eddy currents in the magnet which result from the rapid switching of high gradients, and by self-induction [1]. Moreover the large gradient increases the spectral band width of the imaging experiment to the detriment of the signal-to-noise ratio. For dental materials conventional MRM is restricted to situations in which there is a relatively high concentration of small mobile (diffusing) molecules [2, 3], or when there is partial polymerization [4–6], or when the structure is elastomeric [7, 8].

1.2. Imaging of solids by stray-field nuclear magnetic imaging

Fringe field gradients several tens of Tesla per meter occur at the ends of the superconducting magnet which provides the static field. In 1988 Samoilenko *et al*. [9] proposed using this gradient to obtain high spatial resolution for materials with short T_2 values. This new development in NMR imaging has become known as ''stray-field magnetic resonance imaging'' (STRAFI). The gradient in the stray-field is high enough to spread with high resolution the resonance frequencies of the nuclei. A radio frequency pulse is applied to excite resonance in a narrow slice orthogonal to the gradient. The resulting magnetic intensity is a direct measure of the magnetization in the slice. The thickness of the slice is

$$\Delta r_{\mathrm{p}} = \frac{3^{\frac{1}{2}}\pi}{t_{\mathrm{p}}\gamma g} \tag{2}$$

where Δr_{p} is the slice thickness, t_{p} the pulse length and g the stray-field gradient. Though a long pulse would give improved resolution it is necessary to apply short pulses to observe short T_2 components in the specimen. Since the gradient field is static the specimen is moved mechanically and the pulse reapplied to record the magnetization in the adjacent slice. By stepping the sample through the stray-field the magnetic intensity profile is obtained for the specimen. To avoid overlap the step increment must not be less than the thickness of the excited slice

$$\Delta r_{\mathrm{m}} \geq \Delta r_{\mathrm{p}} \tag{3}$$

where Δr_{m} is the step increment.

In the strong stray-field gradient magnetization decays too rapidly to observe the free induction decay; therefore, the signal is observed in the form of a multiple echo train. The ''quadrature echo'' pulse sequence, which may be written as

$$90_x\ \tau\ (90_y\ \tau\ \mathrm{echo}\ \tau)_n \tag{4}$$

where 90_x is the 90° pulse in the x direction of the rotating frame [10], 90_y the 90° pulse in the y direction of the rotating frame [10], τ the pulse gap and n the number of echoes in the train. This produces a spin-weighted relaxation curve. The pulse length cannot be longer than the pulse gap, which under optimal conditions is of the order T_2. Consequently the best resolution is

$$\Delta r_{\mathrm{B}} = \frac{3^{\frac{1}{2}}\pi}{T_2\gamma g} \tag{5}$$

where Δr_{B} is the slice thickness and T_2 the spin–spin relaxation time. Materials with long T_2 values could produce sub-micrometer resolution. However, long T_2 values are associated with mobile systems which lead to diffusive broadening in the high field gradient and thus limit resolution [11]. For solids with T_2 values between 50 and 100 μs the resolution will be better than 5 μm [12].

At this time (late 1997) fewer than five STRAFI probes exist. In this paper we report on research carried out as part of the UK Science and Engineering Research Council/Industry funded program to investigate the application of STRAFI in materials science research. Dental materials were identified as an aspect of the program for which Dundee would have responsibility and research has been conducted jointly with the University of Surrey, a partner in this inter-university project.

2. Materials and methods

2.1. Materials and specimens

^{1}H is the most studied nucleus for magnetic resonance imaging. It has obvious importance in biological materials, which are ideal subjects for study since they contain a high percentage of water, fats, etc. Imaging of other elements is possible provided an isotope with an uneven number of nucleides is available in high relative abundance, and the element is in sufficient concentration in the material. ^{19}F fulfils the former requirements and dental glass ionomers and their derivatives contain a significant concentration. Developments in restorative materials have resulted in three identifiable fluoride releasing types–conventional glass ionomer, visible light cured glass ionomer, and compomer. One of each was selected for the study (Table I) and for comparison a composite which does not contain fluorine was added to the list.

The specimens were fully cured 5 mm diameter × 9.5 mm length cylinders contained in borosilicate glass tubes. The ends of the Fuji IX specimen were

TABLE I The products used

Product	Manufacturer	Type
Fuji IX	GC Corporation Tokyo, Japan	Glass ionomer
Vitremer	3M Dental Products St Paul, MN, USA	Resin modified glass ionomer
Dyract	Dentsply Detrey GmbH Konstanz, Germany	Compomer
Z 100	3M Dental Products St Paul, MN, USA	Composite

protected with a thin film of light-cured resin. STRAFI measurements were made 7 days after production.

2.2. STRAFI measurements

A STRAFI probe was constructed for use with a 9.4 T, 89 mm vertical bore superconducting magnet. It is a one-dimensional probe to produce data for slices at right angles to the axis of the magnet. A static gradient of $58\ T\ m^{-1}$ exists at the base of this magnet. In this region the field strength is 5.6 T which equates to a resonance frequency of 235 MHz for ^1H. By stepping the specimen through this region with a short, hard 10 μs pulse it is possible to excite resonance in a 40 μm slice. For the present investigation such resolution was not considered essential and a greater stepper increment, 500 μm, was selected.

The ^1H and ^{19}F resonance positions are separated by approximately 6 mm. As the specimen is raised through the stray-field it passes through one resonance position then the other, thus a profile for both elements can be obtained in a single run. At each spatial location (i.e. each step increment) the decay in magnetization was recorded for a train of 16 echoes with a 20 μs pulse gap.

2.3. Solid state NMR measurements

Solid state NMR spectroscopy was applied to the as-received powder and the set cement of Fuji IX to determine whether ^{19}F T_2 values changed as a result of the setting reaction. The magic angle spinning technique (MAS-NMR) was used with a Pencil® rotor spinning at 4 kHz in a 7.05 T, 89 mm bore Chemagnetics CMX300 lite spectrometer (Chemagnetics, Fort Collins, CO). Broad, but usable peaks were produced at the ^{19}F resonance frequency, using a pulse width of 46 μs (90), a pulse delay of 4 s and sweep width of 100 kHz. Data for T_2 determination were collected using a spin echo sequence. Forty points were collected at pulse gap values between 20 and 254 μs. Eight thousand data points were collected for each and transformed with no other manipulation.

2.4. T_2 values

For both STRAFI and solid state MAS-NMR, T_2 values were derived from the magnetization decay by fitting exponential decay curves. In the STRAFI experiment which detects a quadrature echo the decay in magnetization is affected by $T_{1\rho}$ relaxation processes as well as spin-spin relaxation. Consequently the transverse relaxation time values measured during any STRAFI experiment will not be exactly the same as those measured by MAS-NMR. Nevertheless, though the relaxation time which is obtained is not pure T_2 it is still a measure of relative mobility of the atomic species and for the purposes of this paper will be referred to as T_2.

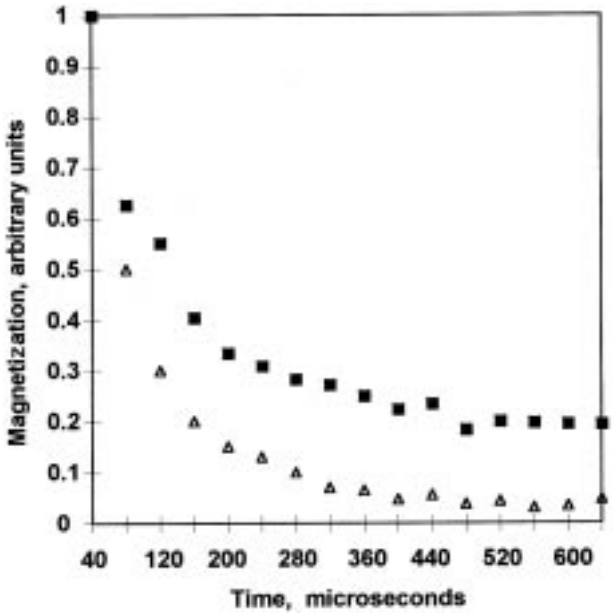

Figure 1 Fuji IX. The magnetization decay of ^1H (Δ) and ^{19}F (■) when a quadrature pulse sequence is applied with a sixteen echo train.

3. Results

Examples of the decays in ^1H and ^{19}F magnetization recorded during the STRAFI experiment are presented in Fig. 1. These follow an exponential law

$$M(t) = M_s \exp -t/T_{2s} + M_L \exp -t/T_{2L} + M_0 \qquad (6)$$

where $M(t)$ is the magnetization at time t, M_s the initial magnetization in the sample due to the component with a short spin/spin relaxation time T_{2s}, t the decay time, M_L the initial magnetization in the sample due to the component with a long spin–spin relaxation time T_{2L}, and M_0 the offset. For ^{19}F a two-exponent curve produced an acceptable fit to the data points. However, for ^1H a single exponent solution proved adequate to fit the signal decays in all four materials.

The T_2 values obtained by STRAFI are listed in Table II. The magnetization values used to calculate both ratios (i.e. total ^{19}F:^1H and $^{19}F_{long}$:$^{19}F_{short}$) are the values obtained by back extrapolation of the exponent curves. ^{19}F T_2 values obtained by solid state MAS-NMR are given in Table III. As expected the STRAFI derived relaxation times are longer than those produced by MAS-NMR. Though a T_2 value obtained by STRAFI for one material should not be compared with a T_2 value obtained by MAS-NMR for a second material both techniques give information which is essentially the same. For a series of materials both techniques produce the same relative values.

An example of an intensity profile, for Fuji IX, is given in Fig. 2. The cylinder length exceeded the distance between the ^1H and ^{19}F resonance positions. This gives rise to the profile in Fig. 2 in which the intensities represent (from the left) ^{19}F alone, ^{19}F and ^1H, and ^1H alone as the cylinder passes through the ^{19}F resonance position but outside the ^1H resonance position, spans both resonance positions, and passed through the ^1H resonance position but is outside the ^{19}F resonance

TABLE II The spin–spin relaxation times, T_2 and the relative intensities of the fluorine to hydrogen signal. Data obtained from the STRAFI experiment

Product	^{1}H T_2 (SD) (μs)	Short ^{19}F T_2 (SD) (μs)	Long ^{19}F T_2 (SD) (μs)	Total F : H intensities (%)	$^{19}F_{long}$: $^{19}F_{short}$ intensities (%)
Fuji IX	183(11)	56(11)	820(220)	23	40
Vitremer	114(11)	50(3)	740(110)	27	35
Dyract	63(3)	54(4)	850(100)	20	32
Z 100	76(6)	No signal	No signal	No ratio	No ratio

NB. Relaxation process other than spin-spin occur and as such these are not pure T_2 values.

TABLE III ^{19}F spin–spin relaxation times, T_2 for Fuji IX. Comparison of values for the as-received powder and the set cement obtained by solid state MAS-NMR (pure T_2) and the set cement by STRAFI

	Short ^{19}F T_2 (μs)	Long ^{19}F T_2 (μs)
Fuji IX powder (MAS-nmr)	33	325
Fuji IX cement (MAS-nmr)	41	664
Fuji IX cement (STRAFI)	56	824

position, respectively. The offset of the ^{19}F resonance plane (displaced 6 mm relative to that of ^{1}H) and the limits of probe movement did not permit the full images of both ^{19}F and ^{1}H to be recorded. The first 3.5 mm of the ^{19}F profile (to the left of that shown in Fig. 2) was not recorded.

4. Discussion

4.1. T_2 values in dental cements

The freedom and mobility of an element (more strictly an isotope of the element) determines the T_2 value [1]. This is reflected in the values for ^{1}H in the four materials. The composite and compomer with polymer matrices have the shortest relaxation times whereas the glass ionomer has the longest. As might be anticipated the resin modified glass ionomer is intermediate.

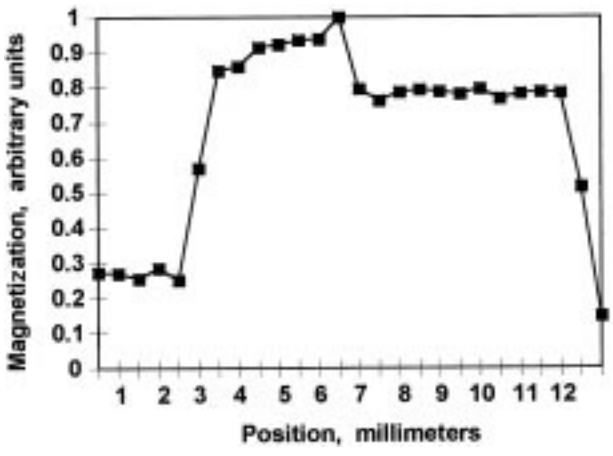

Figure 2 The magnetization in 40 μm slices at right angles to the cylinder axis taken at 500 μm step increments when a quadrature pulse sequence is applied for STRAFI. The end of the cylinder is located at 3.0 mm on the ''Position'' axis. However due to the offset of the ^{19}F resonance plane the ^{19}F image is displaced by -6.0 mm. (The finite length of the probe did not permit the full ^{19}F and ^{1}H profiles to be recorded and the first 3.5 mm of the ^{19}F profile is absent.) As the cylinder is stepped through the stray-field it passes through the ^{19}F resonance position (left plateau), then straddles both ^{1}H and ^{19}F resonance positions (center plateau), then passes through the ^{1}H resonance position alone (right plateau).

For the three products which release fluoride, a short and a long ^{19}F relaxation time were recorded and were similar for all three. Since two values were produced by the Fuji IX powder before setting this result indicates that the fluorine resonances are from the glass and that the element exists in two quite different states in the glass. Fluorine acts as a network modifier in glasses, introducing a non-bridging oxygen into the network which increases the reactivity of the glass. Within the range of glass compositions which produce a dental cement the glass may phase separate or may precipitate a crystalline dispersion (notably CaF_2) during heat treatment [13]. Manufacturers do use heat treatments to adjust the reactivity of the glass. Removal of the fluorine network modifier by precipitation of a compound increases setting time. Wood and Hill [13] note that ''the crystallisation of fluorite occurs relatively easily because Ca^{2+} and F^- ions are mobile in glass networks''. Such mobility would produce a long T_2. In a crystalline structure mobility would be more severely restricted and result in a short T_2. The measurement of a short and a long ^{19}F T_2 is consistent with two phases, i.e. a glass containing a crystalline dispersion. Differences in composition and heat treatment would be anticipated to give glasses with the correct reactivity for three different types of material, more so since they are from different manufacturers located in different countries. Yet the ^{19}F T_2 values are similar. Chemistries may differ but the element must be distributed in two structures.

4.2. STRAFI of the dental cements

Though STRAFI has been used to produce ^{1}H image slices through teeth [14, 15], this is the first reported application of STRAFI to dental materials. The result shown in Fig. 2 is the first reported example of spatially resolved magnetic resonance spectroscopy in a solid dental material or tissue for an element other than hydrogen. There is only one other example of ^{19}F imaging in a solid. As part of his program on multi-nuclear imaging Randall *et al.* [16] used a phantom, consisting of two adjacent polymethylmethacrylate (PMMA) polytetrafluoroethylene (PTFE) discs, to obtain a one dimensional profile similar to that in Fig. 2. It is worth noting that the phantom was carefully chosen as each polymer contains a high concentration of

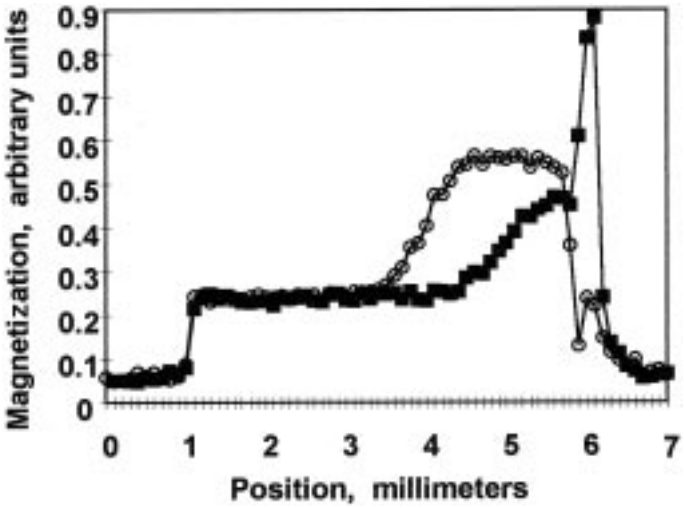

Figure 3 An example to illustrate other STRAFI applications in dental materials research. The magnetization intensity profile for the visible light cured composite product Occlusin® (ICI Dental PLC), shade DY. The curing light has been applied to the end of a 5 mm long × 5 mm diameter cylinder to the left of the profile. ^{1}H profiles for two specimens have been superimposed, ■ 60 s exposure and ○ 20 s exposure to the light. Both monomer and ''fully'' cured polymer produce intensities sufficient to create an image. The cylinder length exceeded the depth of cure for both exposures. (The peaks at the right of the trace are from adhesive used to attach the specimen to the probe. The end of the specimen is at 1.0 mm on the ''Position'' axis.)

only one of the two elements to be detected and none of the other. The present research concerns ''real'' materials with the elements distributed homogeneously through the sample.

STRAFI has been used to produce this one-dimensional profile with a 500 μm resolution, but there is no barrier to extending this to a three-dimensional image with improved resolution. To this end a three-dimensional probe is now being developed. The importance of the research reported in this paper is the demonstration that fluorine MRM of dental solids is feasible through STRAFI.

4.3. Other applications of STRAFI in dental materials research

STRAFI is non-destructive and the high natural abundance of a suitable isotope (^{19}F) will allow the application of the technique to a variety of dental problems. For example, following the release of the element from a dental cement into the surrounding tooth by three-dimensional imaging. One dimensional profiling using surface coils and frequency sweeping is more appropriate for a second example, studying the interface between glass and polyalkenoic acid over time as the two components react. ^{1}H STRAFI imaging will find extensive application. Two of these will be reported in detail in subsequent papers, depth of cure and diffusion of liquids into the polymer. To illustrate this an example of a depth of cure profile is shown in Fig. 3.

STRAFI has an advantage over MRM as it is able to image both monomer and polymer. However, while STRAFI can image liquids diffusing into dental diacrylate resins to a resolution of 24 μm it cannot differentiate individual liquids in homogeneous mixtures as can MRM. STRAFI and MRM must therefore be considered as complementary techniques to be used as appropriate to the problem being investigated.

Acknowledgment

This research was funded by EPSRC (UK) grant GR/K 12397. We gratefully acknowledge the donation of materials by the manufacturers listed in Table I.

References

1. W. KUHN, *Angew. Chem. Int. Ed. Eng.* **29** (1990) 1.
2. C. H. LLOYD, S. N. SCRIMGEOUR, J. A. CHUDEK, G. HUNTER and R. L. MACKAY, *Plast. Rubber Comp.* **24** (1995) 181.
3. P. JEVNIKAR, J. OREST, A. SEPE, M. M. PINTAR and N. FUNDUK, *Dent. Mater.* **13** (1997) 20.
4. C. H. LLOYD, J. A. CHUDEK and G. HUNTER, *J. Dent. Res.* **70** (1991) 713.
5. C. H. LLOYD, S. N. SCRIMGEOUR, J. A. CHUDEK, G. HUNTER, R. L. MACKAY, D. PANANAKIS and E. W. ABEL, *Dent. Mater.* **10** (1994) 128.
6. S. N. SCRIMGEOUR, C. H. LLOYD, J. A. CHUDEK and G. HUNTER G., *J. Dent. Res.* **71** (1992) 720.
7. A. D. GILBERT, C. H. LLOYD and S. N. SCRIMGEOUR, *J. Periodontol.* **65** (1994) 324.
8. C. H. LLOYD, S. N. SCRIMGEOUR, J. A. CHUDEK, G. HUNTER and R. L. MACKAY, *Quintessence Int.* **28** (1997) 349.
9. A. A. SAMOILENKO, D. YU. ARTEMOV and A. L. SIBEL'DINA, *JETP Lett.* **47** (1988) 348.
10. P. T. CALLAGHAN, in ''Principles of nuclear magnetic resonance microscopy'' (Clarendon Press, Oxford, 1991).
11. P. J. MCDONALD, *Prog. Nucl. Magn. Reson. Spect.* **30** (1997) 69.
12. P. M. GLOVER, P. J. MCDONALD and B. NEWLING B, *J. Magn. Res.* **126** (1997) 207.
13. D. WOOD and R. HILL, *Biomaterials* **12** (1991) 164.
14. M. A. BAUMANN, D. GROSS, V. LEHMANN and K. ZICK, *Schweiz. Monatsschr. Zahnmed.* **103** (1993) 1407.
15. M. A. BAUMANN, G. M. DOLL and K. ZICK, *Oral. Surg. Oral. Med. Oral. Pathol.* **75** (1993) 517.
16. E. W. RANDALL, A. A. SAMOILENKO and T. NUNES, *J. Magn. Res.* **A117** (1995) 317.

Received 28 January
and accepted 3 August 1998